Interaction Notes
Note 544

May 1998

STATISTICAL RESPONSE OF EM-DRIVEN CABLES INSIDE AN OVERMODED ENCLOSURE[1]

Richard Holland and Richard St. John
Shield Rite, Inc., P. O. Box 8250, Albuquerque, NM 87198, (505) 842-6018

Abstract

This paper deals with probabilistic modeling of the EM response of cables inside a complex cavity subjected to well-overmoded EM penetration. Theoretical studies indicate that the field amplitudes and cable currents squared both should have a chi square distribution with two degrees of freedom, but our observations indicate that a log normal fit is empirically better unless the data, if experimentally obtained, is first passed through a carefully tailored trend-removing filter. If a cable model is driven by statistically simulated enclosure fields, similar extreme care must be taken with the numerical generation of these driving fields. The major innovation reported here is the development of a Monte-Carlo algorithm which models cable-drive fields simultaneously having a chi square power flux distribution, and the physically mandated local autocorrelation at a spatial point as frequency is swept or at a fixed frequency as the power flux sensor is moved around to map the cavity response. Nature is quite adept at creating a cable drive with these simultaneous attributes, but computer emulation had proved very exasperating. Our algorithm, as an unplanned bonus, also has the capability to transform random numbers from one distribution to another. For instance, one can input normally distributed power flux values and obtain as the output chi square or log normally distributed power flux values. The reverse transformations are also allowed.

---

[1] This work was supported by the U. S. Air Force Phillips Laboratory under Contract F29601-94-C-0061.

Interaction Notes
Note 544

September 1998

STATISTICAL RESPONSE OF EM-DRIVEN CABLES INSIDE AN OVERMODED ENCLOSURE[1]

Richard Holland and Richard St. John
Shield Rite, Inc., P. O. Box 8250, Albuquerque, NM 87198, (505) 842-6018

Abstract

This paper deals with probabilistic modeling of the EM response of cables inside a complex cavity subjected to well-overmoded EM penetration. Theoretical studies indicate that the field amplitudes and cable currents squared both should have a chi square distribution with two degrees of freedom, but our observations indicate that a log normal fit is empirically better unless the data, if experimentally obtained, is first passed through a carefully tailored trend-removing filter. If a cable model is driven by statistically simulated enclosure fields, similar extreme care must be taken with the numerical generation of these driving fields. The major innovation reported here is the development of a Monte-Carlo algorithm which models cable-drive fields simultaneously having a chi square power flux distribution, and the physically mandated local autocorrelation at a spatial point as frequency is swept or at a fixed frequency as the power flux sensor is moved around to map the cavity response. Nature is quite adept at creating a cable drive with these simultaneous attributes, but computer emulation had proved very exasperating. Our algorithm, as an unplanned bonus, also has the capability to transform random numbers from one distribution to another. For instance, one can input normally distributed power flux values and obtain as the output chi square or log normally distributed power flux values. The reverse transformations are also allowed.

---

[1] This work was supported by the U. S. Air Force Phillips Laboratory under Contract F29601-94-C-0061.

Introduction

This paper reports accomplishments in statistical modeling of the electromagnetic (EM) field and cable response of an enclosed system in the presence of radio frequency (RF) leakage and penetration. The problem of predicting cable or pin currents in an enclosed, leaky system under RF illumination or other RF interference (RFI) at a frequency where the enclosure is many (>6) wavelengths on a side (i.e., well overmoded) is all but impossible to solve deterministically. Moreover, even assuming a supercomputer and state-of-the-art finite-volume time-domain (FVTD) code were available, one could logically claim a deterministic solution would be of no value. This claim could be made because, in such a scenario, a 1° rotation of the enclosure or a 1 percent shift in frequency could alter the response at any given pin or circuit device by 20 dB. Additionally, the interior of a satellite, aircraft, or missile has wiring of almost inconceivable complexity as viewed by an FVTD practitioner who is used to zero or one (two if he is really heroic) conductors passing through each FVTD cell.

To solve this sort of problem deterministically, one not only needs to track the fields in 10^6 to 10^9 FVTD cells, but also to model the drive these fields impose on each conductor (or even each IC) passing through or located in each cell. The final nightmare is that each of these conductor and IC currents must then be fed back through the FVTD version of the curl $\boldsymbol{H}$ equation (Ampere's law) to drive the algorithm which advances the FVTD field solution. Despite 25 years' experience with FVTD and finite-difference time-domain (FDTD) codes, it is our conviction that this problem is at least two computer generations from tractability, even assuming a deterministic solution could be of any use.

Given this dark and bleak outlook on deterministic analysis, the RFI community was thoroughly awakened by a statistical approach worked out by Price and Davis which appeared in 1988.[1,2] A statistical treatment, unlike a deterministic treatment, actually thrives on complexity. In many situations, the statistical confidence interval depends on the *inverse* square root of the amount of data provided.[3,4] The statistical approach develops a probability density function model for the fields inside an enclosure which is not a hair-trigger function of frequency, illumination angle, wiring configuration, or any other parameter. The most elementary probabilistic models use the assumption that the distribution of electric or magnetic field squared (i.e., power flux projected on a dipole antenna's cross-section) are chi square distributed with two degrees of freedom; i.e., exponentially distributed. This distribution is characterized by a single parameter, μ the mean value.[1,3]

In this paper, we work out relationships for determining the statistics of the driving fields to apply to a circuit analysis code representing part of an enclosed system's wiring. This modeling must be achievable from a very minimal amount of information, such as just the empirically observed average power flux or dipole antenna energy pickup in the enclosure of interest. We also address other aspects, such as limited spatial and frequency coherence, which a statistically based field drive model must have. After all, there is some small distance Δr and some small frequency shift $\Delta\omega$ below which the RFI response at a wire or pin in the enclosure will not change

significantly. It proves to be non-trivial to generate field models which simultaneously include the proper field distribution and coherence.

Statistical and Empirical Background

The cable power or EM field power flux versus frequency plot made by a sensor inside a resonant, overmoded cavity will, in general, look like the highly irregular lower curve in Figure 1. There are two classes of factors which contribute to the fluctuation seen in this sort of measurement. The first are slowly varying effects or "trends", such as frequency-dependent Q inside the cavity and cable attenuation in the measuring setup. The second are rapidly varying effects, such as a 1% frequency shift causing the sensor position with respect to the standing wave pattern to shift from a field or current peak to a field or current null. The same distinct types of fluctuation occur if sensor position instead of illuminating frequency is the independent variable. The trend on a data set obtained as Figure 1 corresponds approximately to the slowly varying spatial function $g(r')$ introduced by Price and Davis [1,2] at their Eq. (5). It also corresponds to the field nonuniformity observed by Hill [5] in a stirred-mode reverberation chamber, and shown in his Figures 8 and 9. (We have not personally worked with data where the driver or observer position changes, although this sort of study was reported in [5].) In this article, we are only interested in effects and statistics of the second class of fluctuations. Separating or factoring the trend from the rapid fluctuation is

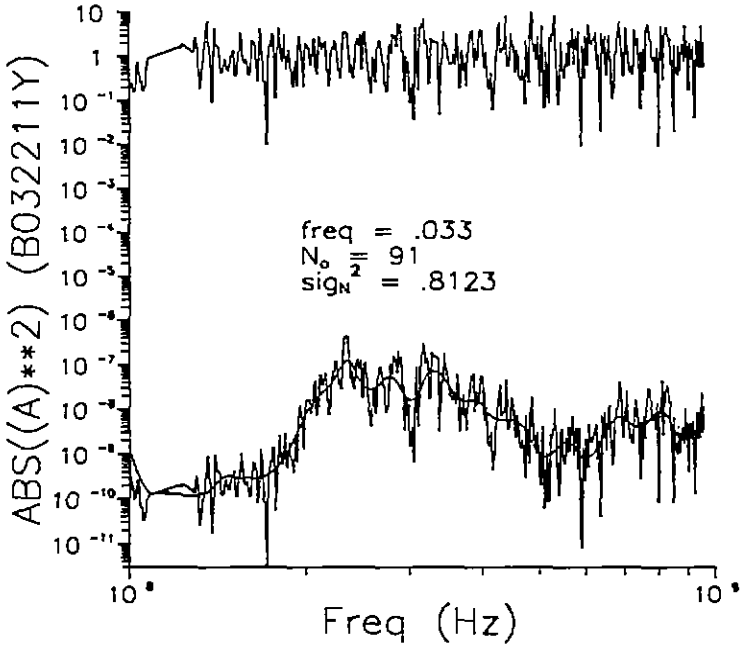

Figure 1. Cable current squared (power) as seen on a cable inside an enclosure (the EMPTAC aircraft shell) illuminated by overmoding conditions.

referred to as "detrending". We implement it as follows:[6]

Start with the data array P_n ($n = 1,... N$). Let L_n be the $\log_e$ of P_n. Then, convolve the L_n array with a truncated filter of the form $C_n = (\sin \alpha n)/(2\pi\alpha n)$, where the truncation is symmetrically set to include the central lobe of C_n and two sidelobes (the first positive-going and the first negative-going) in each direction. Let us imagine for a moment that the data is actually a function of time (not frequency), with each point separated by 1 s. Let N_0 be the number of points inside or at the truncation limits of C_n. Then convolution of the L_n array with the C_n array corresponds to passing L_n through a low-pass filter of cutoff frequency $f_{co} = 3/(N_0 - 1)$. The low-pass convolution output is the trend of L_n, M_n. The smooth lower curve in Figure 1 represents $\exp(M_n)$, the trend of the original array. Thus, $(L_n - M_n)$ is the detrended data array in the $\log_e$ domain, and $P_n' = \exp(L_n - M_n)$ is the actual detrended data, which is represented by the upper irregular curve of Figure 1. Note that the original lower, rapidly varying curve in Figure 1 is the product of the upper curve and the lower smooth curve. For the Figure 1 data set, we empirically found 91 to be the best value for N_0; this corresponds to $f_{co} = 0.033$. The variable α is then adjusted so $\alpha(N_0 - 1) = 3\pi$; i.e., $\alpha = 0.1047$. The optimum value of N_0 might be expected to vary dramatically from experiment to experiment, and to depend strongly on how every data set is obtained. We have, somewhat to our surprise, however, found $N_0 = 91$ to work well on data sets of all experiment types (four enclosed systems) we have sought to detrend.

This concurrence of $N_0 = 91$ for four different experiments is probably serendipitous. On the other hand, a highly skilled experimentalist may (pardon us) have an intuitive feel for how densely to sample data so that nothing is lost, but also nothing extraneous is recorded, and may subconsciously or deliberately set his recording equipment so $N_0 = 91$ is consistently optimum for detrending power flux data taken at just the right spacing.

There exist rationale and precedent for dealing with the log arrays, as opposed to the original arrays. For instance, if $\{u_n\}$ is a chi square ensemble with two degrees of freedom, then $\mathrm{Var}\{\ln(u_n)\}$ is always $\pi^2/6$.[7] Thus, taking the variance of a log array is a simple test to reveal whether the original array is, at least by one standard, approaching chi square. In Figure 1, the quantity σ_N^2 is given. This is the variance of the filtered $\{\ln(u_n)\}$
array normalized by $\pi^2/6$. Aside from a somewhat subjective examination, the selection of an optimum N_0 associated with the filtering of a family of data sets is determined by choosing a value which makes the average σ_N^2 of all the data sets in the family closest to unity.

In a simple, ideal world, we would like not to have to remove trends. It has been established that, if we could devise an experiment with trends absent, the power picked up by a dipole antenna in an overmoded cavity would obey a chi square distribution with two degrees of freedom. (At present, we *do* know how to deal with trends, but this subject is beyond the introductory material we are presenting in this paper.) This statement is true under cw conditions, and would apply whether the observations are made at a fixed observation point while frequency is swept or whether the observations are made at a fixed frequency while the sensor probe is translated or rotated.[1,2,6,8] It also appears to be true for a mode-stirred reverberation chamber where the paddle angle is the

independent variable.[9-11] As already discussed, however, this ideal result depends on the cavity not having a frequency-dependent Q and on all parts of the cavity being equally shielded (i.e., no subenclosures within the enclosure, no regions with closely spaced walls which could act like a waveguide below cutoff, and no field observations made at points significantly illuminated by direct radiation from the driving source). If these postulates are not obeyed, the received antenna power distribution usually appears log normal instead.[6,8].[2]

In general, for real-world problems, conditions are not ideal, and the dipole antenna response contains a "trend", as well as a rapidly varying response associated purely with the electromagnetic statistics. Then it becomes necessary to filter out this trend if one wishes to see the chi square statistical behavior [6,8]. Price, *et al.* [1], have published a thorough derivation of the physics and statistics responsible for the chi square attribute of the squared fields (power flux). However, there is a simple approach which relies somewhat on intuition for reaching the same conclusion. Essentially, at any point in the enclosure, the field projected on any dipole consists of two components in phase quadrature, each of which approaches a normal distribution when the enclosure is sufficiently overmoded to begin to have blackbody-like characteristics. (This distribution is a consequence of Bose-Einstein statistics, which describe blackbody radiation.) The power picked up by a dipole antenna is proportional to the summed squares of these quadrature components. (Alternatively, it could be viewed that the power picked up is the summed squares of the waves going backwards and forwards.) However, this sum is exactly the definition of a function which has a chi square distribution with two degrees of freedom.

(Reference [1] originally appeared as a corporate memorandum [2], which has become somewhat of a classic opus despite its initially invisible release. Unfortunately, both [1] and [2] drop a $V_{ph}(r')$ in the denominator of their Eq. (7), which is never picked up, and renders much of their following work not even dimensionally correct. Their conclusion about power flux having a chi square distribution with two degrees of freedom is not impacted by this error, however.

(Another publication by Hill, *et al.* [13], presents a nice summary of the interior responses of aperture-driven chambers as they relate to easily accessible electromagnetic quantities, such as

---

[2] Almost any data set which depends on a bunch of somewhat random factors will have an approximately log normal distribution. This approximate relationship may be inferred from the Central Limit Theorem. If each of the random factors has an identical distribution, the approximate relationship becomes precise. To be more specific, any sum of M variates u_m, $m = 1,...M$ where $E\{u_m\}$ and $Var\{u_m\}$ exist will itself converge to a normal distribution as M goes to infinity. (Cauchy's distribution [4,12] is an example where $E\{u_m\}$ and $Var\{u_m\}$ do not exist, and where a sum of variates does not converge to a normal distribution.) Consequently, the log ensemble of a data set with a bunch of random factors, where each factor has the same distribution, will approach a normal distribution, as the log operator converts the product of factors to a sum of components. This means the original data set itself will have a distribution which is (approximately) log normal. To be even more general, if the different variates making up a sum all have different distributions but with $E\{u_m\}$ and $Var\{u_m\}$ existent for each variate, the Central Limit Theorem still applies, even if the individual variate distributions themselves are different. [12]

the chamber volume V and Q. This paper is much lighter reading than the Price work [1,2], as it is closer to being deterministic, with concise engineering approximations, and does not bog down with tedious probabilistic expectation derivations.)

An empirical result we have observed about data pertaining to the power (current squared) carried by a cable inside an enclosure is that it *also* obeys a chi square distribution with two degrees of freedom after the power is detrended (see the probability plot of Figure 2).[3] However, if the power is viewed as the summed squares of two phase quadrature currents, there is no surprise in this observation. (There is an experimentally prompted assumption here that the unsquared phase quadrature current components also have a normal distribution. In this case, however, this assumption is merely *ad hoc*, and we do not claim our simplistic appeal to Bose-Einstein EM field statistics extends to cable currents.)

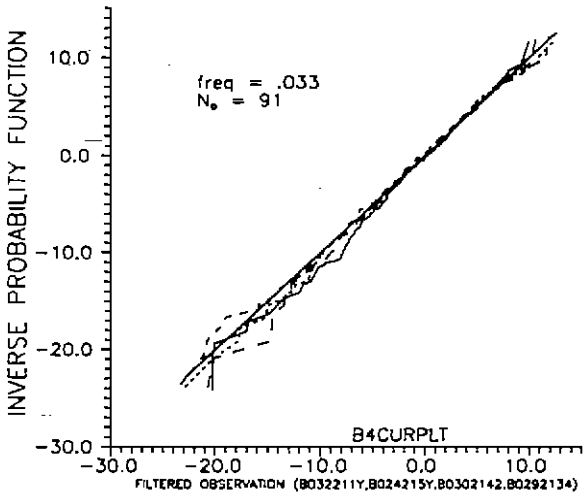

Figure 2. Probability plots of observed, trend-removed EMPTAC cable powers show good fit vs a χ^2 distribution. See Footnote 3.

---

3 A probability plot is a means of comparing an assumed distribution with an observed data set. Let us hypothesize that the assumed cumulative distribution is defined as $p = \Phi(w)$, meaning a fraction p of the points in the data set have value w or smaller. Let there be N points in the data set. Let the data set be ordered so the nth smallest value has index n. Then evaluate $\Phi^{-1}((n-\frac{1}{2})/N) = U_n$. Make a dot at W_n on the horizontal (observed data) axis, and at U_n on the vertical (assumed inverse probability function) axis. If $\Phi(w)$ is the correct distribution, all N of the dots will then lie close to a 45° line, where the individual point deviation of the dots from this line goes to zero as the number of points goes to infinity. It is also possible to perform confidence tests, of which the Kolmogorov-Smirnov test [3] is probably the best, which bound the 45° line with upper and lower confidence curves [1,2]. The spacing between these bounds with respect to the 45° line diminishes in inverse proportion to the square root of the number of points in the data set.

The Chi Square Distribution with Two Degrees of Freedom

In particular, if we have a cable inside an enclosure carrying a sinusoidally varying current with u and v the current phase quadrature components, the cable power will be of the form

$$z = x + y = u^2 + v^2 \tag{1}$$

In many actual situations, we can measure empirically the probability density function of z, which we denote $h(z)$. From $h(z)$, we need to back out the probability density functions of x and y. This can be done as follows: define the Fourier transform $H(\omega)$ of $h(z)$ as

$$H(\omega) = \int_{-\infty}^{\infty} h(z) e^{-j\omega z} dz \tag{2}$$

where, in probability terminology, $H(\omega)$ is the characteristic function of the distribution of z.[3,12] If x and y are statistically independent, it can be shown that the probability density function $h(z)$ is related to the probability density functions of x and y, $f(x) = f(y)$ by

$$h(z) = \int_{-\infty}^{\infty} f(x) f(z - x)\, dx \tag{3}$$

so that $f(x)$ is related to $h(z)$ by

$$f(x) = \frac{1}{2\pi} \int_{-\infty}^{\infty} [H(\omega)]^{1/2} e^{j\omega x} dz \tag{4}$$

where care must be taken in evaluating the square root in (4) by placing the complex-plane branch cuts so as to give physically meaningful results.

In general, if u and x are related by the transformation function

$$u = g(x) \tag{5}$$

where, if $g(x)$ is a single-valued, monotonically increasing function, the probability density functions of u and x are related by

$$e(u) = f(g^{-1}(u)) \frac{dg^{-1}(u)}{du} \tag{6}$$

This last relationship is generally true if the underlying distribution of z is anything reasonable (i.e.,

chi square, normal, or log normal). If $g(x)$ is a multiple-valued function, as is the case here

$$g(x) = \pm (x)^{1/2} = u \tag{7}$$

(x must be positive, but u is bipolar), (6) must be modified so $e(u)$ implies a symmetric probability density function over its positive and negative branches, while still having an integral of unity over its entire range, $-\infty < u < \infty$

$$e(u) = \begin{cases} \frac{1}{2} f(g^{-1}(u)) \dfrac{dg^{-1}(u)}{du} & u > 0 \\ \frac{1}{2} \left| f(g^{-1}(u)) \dfrac{dg^{-1}(u)}{du} \right| & u < 0 \end{cases} \tag{8}$$

In the special case of z having a chi square distribution with two degrees of freedom, we have

$$\begin{aligned} h(z) &= e^{-z/\mu_c}/\mu_c & z > 0 \\ &= 0 & z < 0 \end{aligned} \tag{9}$$

and we find, from (2)-(4) and a bit of symbol manipulation which is moderately easy to work out, but is set down in [14], that $f(x)$ can be evaluated in closed form,

$$f(x) = \frac{1}{\sqrt{\pi}} \frac{e^{-x/\mu_c}}{\sqrt{x\mu_c}} \tag{10}$$

and, thus, $e(u)$ becomes

$$e(u) = \frac{1}{\sqrt{\pi}} \frac{e^{-u^2/\mu_c}}{\sqrt{\mu_c}} \tag{11}$$

In (9)-(11), μ_c is the mean of z.

We thus see that, if the cable power (current squared) obeys a chi square distribution with two degrees of freedom, the phase quadrature components have a normal distribution with zero mean,

$$e(u) = \frac{1}{\sqrt{2\pi}} \frac{e^{-u^2/(2\sigma_g^2)}}{\sigma_g} \tag{12}$$

where the μ_c (the mean of z) and σ_g (the standard deviation of u) are related by

$$\mu_c = 2\sigma_g^2 \tag{13}$$

(Statistical parameters relating to a chi-square distribution are subscripted with a c, while those relating to a normal or Gaussian distribution are subscripted with a g.)

Forcing of Autocorrelation

If a cable is within $\lambda/2$ of a conducting wall, the drive per unit length on the cable is a zero-impedance voltage source per unit length of value

$$E_{dr} = -\mu_0 h \frac{dH_{tr}}{dt} \tag{14}$$

where h is the separation between the wall and the cable centerline, and H_{tr} is the component of the surface current density on the wall flowing parallel to the cable. H_{tr} is related to the fields in the center of the cavity by $H_{tr} \approx \sqrt{2}\, H$. This relationship is based on energy considerations and differs from the factor of 2 seen for specular reflection of a plane wave.

Test data referenced here (see Figure 1) was obtained at the Air Force Research Laboratory's (AFRL) EMP effects EMPTAC [EMP Test AirCraft] facility. The EMPTAC is essentially a gutted 720 airframe with interior dimensions resulting in an f_{111} of around 20 MHz; illumination of the cavity at frequencies above 100 MHz ensures the results are those of an overmoded cavity. Excitation of the EMPTAC interior is by external illumination (using the AFRL Laboratory's Ellipticus Antenna) with EM energy leaking in through deliberate and inadvertent apertures, and by antenna feed cables. Before detrending, EMPTAC cable powers and EM power flux densities tend to appear log normal in distribution. The squares of the time-derivative of B were actually measured. Subsequently, a signal processor performed integrating corrections to reverse the derivative effect and also performed other manipulations to correct for frequency dependence of the probe. At no time was phase information obtained.

Our first attempt to model the effects of a chi square power distribution incident on a cable was performed by constructing a transmission-line computer model based on the cable physically tested in the EMPTAC. The computerized transmission-line model and the actual EMPTAC cable were both terminated in their characteristic impedance (about 30 Ω). Also, the model cable length, 20 m, was selected to approximate the actual EMPTAC cable length. Similarly, in the computer model, the cable standoff h approximated the standoff of the actual EMPTAC cable standoff, $h = 5$ cm. (No modeling was attempted of the sightly irregular standoff present in the real EMPTAC cable.) The cable transmission-line model was given an inductance per unit length L of 1 μH/m, and a corresponding capacitance per unit length C which would cause propagation at c. For the computer model, the cable was divided into 200 segments, the ith denoted by i, $i = 1...I = 200$, and excited at 1000 different frequencies the nth denoted by n, $n = 1...N = 1000$, exponentially stepped between 100 MHz and 1 GHz. The phase quadrature magnetic driving fields on each segment were randomly

chosen variables from a normal distribution with a zero mean and a standard deviation of 0.01 A/m. (This value was selected for σ_g in view of (13), as we had experimental EMPTAC magnetic-field data for μ_c typically placing it around 2×10^{-4}.) In particular, each cable model segment was driven by a random field of the form

$$H_{tr}(n,i) = [A(n,i) \cos \omega_n t + B(n,i) \sin \omega_n t] \quad \textbf{(15)}$$

where $A(n,i)$ and $B(n,i)$ were obtained from

$$(A \text{ or } B)(n,i) = \sigma_g u(n,i) \quad \textbf{(16)}$$

with $\sigma_g = 0.01$ and $u(n,i)$ evaluated from a Monte Carlo simulation designed to give a variate with normal distribution with unity standard deviation and zero offset:

$$R(n,i) = \frac{1}{\sqrt{2\pi}} \int_{-\infty}^{u(n,i)} e^{-t^2/2} dt \quad \textbf{(17)}$$

Here, $R(n,i)$ is a random number uniformly distributed from 0 to 1. Also, i is the cable segment index, n is frequency index of ω_n, and the random number $R(n,i)$ used to obtain $A(n,i)$ is completely uncorrelated with that used to obtain $B(n,i)$ [so that (3) and (4) apply]. Equation (14) was then used to convert the magnetic driving field into the actual driving electric field in the model's transmission line equations.

Unlike actual experimental data, application of (17) did not result in a cable power distribution which was chi square, even after filtering for trend removal. The problem was the $A(n,i)$ or $B(n,i)$ generated in this manner had no local autocorrelation, either between adjacent frequencies or between adjacent cable segments. Thus, the resulting simulated cable powers, unlike the experimentally observed EMPTAC cable powers (see Figure 3), also had no autocorrelation between adjacent frequencies. (It turns out that we don't know how non-iteratively to generate an ensemble of drivers which simultaneously and automatically has a prescribed probability density function *and* autocorrelation. Nature does this for us with the experimentally generated real-world drivers, but in our virtual reality, we here have a very difficult time replicating nature.)

It is known that the spatial autocorrelation of any component of the fields (with frequency fixed) should depend on the separation of the two observational points, $\Delta r = |r_1 - r_2|$, as [15-17]

$$\rho(r_1, r_2) = \frac{\sin(k|(r_1 - r_2|)}{(k|r_1 - r_2|)} \quad \textbf{(18)}$$

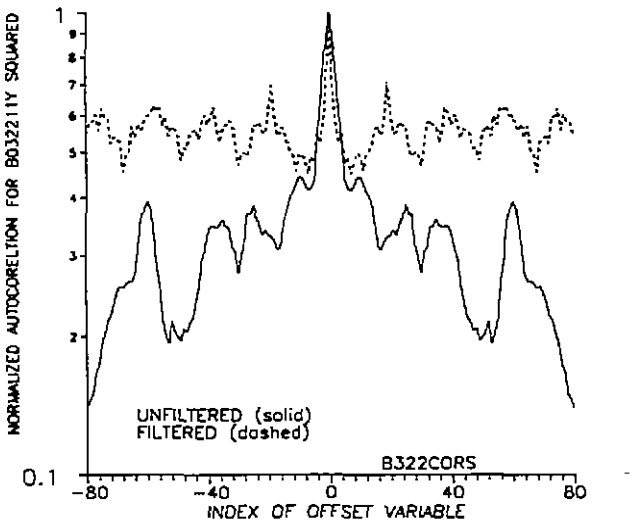

Figure 3. The EMPTAC cable power has a central peak several frequency steps wide in its frequency autocorrelation.

and the frequency autocorrelation (with observer position fixed) should depend on the spectral separation of the two frequencies, $\Delta\omega = \omega_1 - \omega_2$, as [16]

$$\rho(\omega_1, \omega_2) = \frac{1}{1 + \beta(\omega_1 - \omega_2)^2 Q^2} \tag{19}$$

where β is a constant which depends in a complex way on the chamber dimensions. However, we re-emphasize that knowing what the autocorrelation and distribution of the electromagnetic fields should be does not trivialize their computerized simulation.

The first attempt to rectify this problem and to introduce autocorrelation consisted of massaging the $u(n,i)$ given by (17). With the Monte Carlo $R(n,i)$ still a random number uniformly distributed between 0 and 1, we associated a $u_{lim}(n,i)$ with each $R(n,i)$ through (17), setting $u(n,i) = u_{lim}(n,i)$.

We then defined an intermediate new $u(n,i) = u_{space}(n,i)$ through a formula empirically selected from a half dozen possible choices to force spatial autocorrelation between nearest-neighbor segments

$$u_{space}(n,i) = \frac{\frac{\lambda_n}{\Delta l} u(n,i-1) + f_{space}\, u_{\lim}(n,i)}{\frac{\lambda_n}{\Delta l} + f_{space}} \tag{20}$$

where $u(n,i-1)$ is the $u(n,i)$ for the previous cable segment $i - 1$, Δl is the cable segment length, and

f_{space} is a number around 10. (Actually, this selection is not totally empirical: it has the desired property that, for cable segment length constant, coherence between segment drives is high at long wavelengths, but decreases as wavelengths become small, with the turn-over point occurring around $\lambda_n = \Delta l$.) At the left end of the cable, $u(n,1)$ was seeded as ½. Making f_{space} zero results in total correlation between adjacent segments; making it >1000 results in no noticeable correlation between adjacent segments; i.e., no change between $u_{lim}(n,i)$ and $u_{space}(n,i)$ closely approaching the EMPTAC experimental noise floor. We then obtained a new $u(n,i) = u_{freq}(n,i)$, locally autocorrelated over both space and frequency, through a formula to force autocorrelation between adjacent frequencies

$$u_{freq}(n,i) = \frac{\frac{\lambda_n^2}{L(\Delta\lambda)_n} u(n-1,i) + f_{freq}\, u_{space}(n,i)}{\frac{\lambda_n^2}{L(\Delta\lambda)_n} + f_{freq}} \qquad \textbf{(21)}$$

Here $u(n-1,i)$ is the $u(n,i)$ for the previous frequency $n-1$, L is the linear dimension of the cable extent, $\Delta\lambda$ is the change in wavelength between adjacent frequencies, and f_{freq} is another number around 10. [At the lowest frequency, $u(1,i)$ was again seeded as ½. Making f_{freq} zero results in total correlation between adjacent frequencies; making it >1000 results in no noticeable correlation between adjacent frequencies. The actual $u(n,i)$ used for cable drive in (15) and (16) is, in the first approximation, $u_{freq}(n,i)$ of (21).]

This procedure succeeds in introducing an approximate simulation of the physically occurring autocorrelation in cable power over position and frequency (compare Figure 4 with Figure 3). Unfortunately, it also succeeds in distorting the normal distribution that we desire the array of $u(n,i)$'s to possess, especially at the tails (see Figure 5). Additionally, the standard deviations σ_g, i.e.,

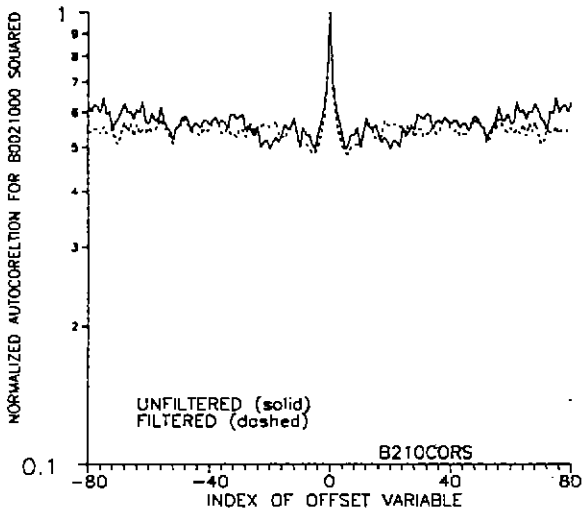

Figure 4. Numerically simulated cable power autocorrelation after forcing autocorrelation onto cable drivers.

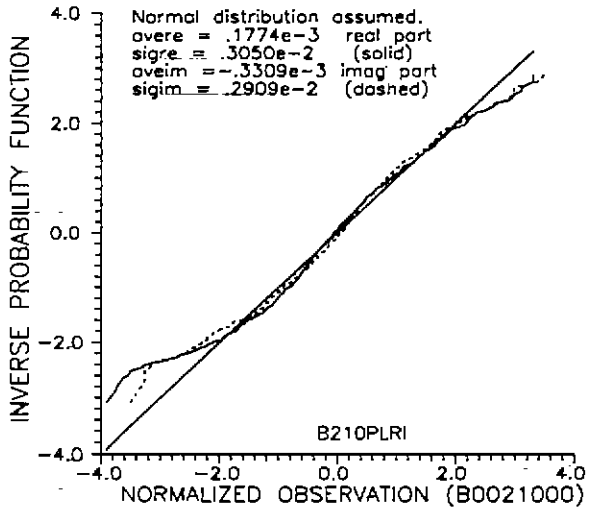

Figure 5. Forcing autocorrelation on the driver ensembles makes distribution tails non-normal and reduces σ by ~.3.

average amplitudes of the driver ensemble matrices $u(n,i)$ and $v(n,i)$, are reduced from .01 to about .003.

Restoration of the Normal Distribution

The normal distribution of the $u(n,i)$ may be realized along with an approximate satisfaction of the desired autocorrelation attributes of (18) and (19) by the following process: Let us begin by generating the two-dimensional ensemble or matrix of numbers along the spatial and frequency axes according to (16)-(21). [Actually, we need two ensembles, one of which will eventually become $A(n,i)$ of (15), and the other of which eventually will become $B(n,i)$.] Then pick a particular spatial point or cable segment i and examine the one-dimensional array or sequence which characterizes the drive versus frequency at this point. To the element of this sequence having the lowest value, assign the index $m = 1$; to the next, assign $m = 2$; etc.; up to $m = m_{max} = N$.

In general, the elements of this array (and even the elements of the array of indices m listed versus frequency) will be in a sequence containing autocorrelation information, but the actual values of the elements of this array will have been speciously altered away from a normal distribution in the process of introducing the autocorrelation [(19) and (20)]. We shall now reverse this alteration without destroying the autocorrelation by utilizing the concept that even the array of indices m contains some residual autocorrelation information.

Let us associate a fraction with each point in the one-dimensional array:

$$f_m = (m - \tfrac{1}{2})/m_{\max} = (m - \tfrac{1}{2})/N \qquad (22)$$

If, for fixed spatial position i, this array actually had a normal distribution with zero mean and σ_g variance, it would be true that, if $u(m,i)$ were the value of element m,

$$\Phi_g(u(m,i)/\sigma_g) = f_m \qquad (23)$$

where $\Phi_g(u(m,i)/\sigma_g)$ is the cumulative normal probability distribution function. Since this should be true, we shall force it to be true: Rescale each $u(m,i)$ to obey

$$u(m,i) = \sigma_g \Phi_g^{-1}(f_m) \qquad (24)$$

where $\Phi_g^{-1}(f_m)$ is the inverse of the normal cumulative probability distribution function.

Note that this rescaling does not undo the autocorrelation because the m's themselves contain some autocorrelation along the frequency axis. (Very negative numbers tend to be adjacent to other very negative numbers, etc.) It is interesting to point out that this procedure can be used to transform the $u(m,i)$'s into an array with any desired distribution, irrespective of the underlying initial

distribution used to find $u_{lim}(m,i)$ in (17). For instance, if $\Phi_g^{-1}(\ )$ of (24) is replaced by the inverse chi square or log normal cumulative distribution function, the $u(m,i)$'s emerging from (24) will become chi square or log normal in distribution.

The following observations now seem in order:

1. This rescaling procedure must, of course, be repeated for the 1D array at each of the spatial drive points.
2. Autocorrelation also existed along the spatial axis before rescaling by virtue of (20) and (21). Since we merely rescale, not resequence, this rescaling will also preserve this autocorrelation along the spatial axis.
3. If we impose a rescaled normal distribution on the $u(n,i)$'s along the frequency or n axis, and if this rescaled distribution is obtained in the same manner for each spatial point, the distribution of a 1D array taken in the *other* direction along i (frequency constant, spatial position variable) will also approach a normal distribution as the number of spatial and frequency observation points both become large.
4. In this entire operation of rescaling the 2D ensemble, there is no reason we cannot reverse the roles of the frequency and the spatial axes across the ensemble.
5. Even if the problem is extended to three spatial (and one frequency) dimensions, rescaling needs to be done only in one direction.

Now let us reinforce some of these ideas with results. A normal random-distribution generating process set to give zero mean and 0.01 standard deviation was used to initialize all the ensembles which follow. Likewise, f_{space} and f_{eq} were always set to 10, [which gives a fair approximation to the autocorrelation actually observed in the EMPTAC test data we are trying to mimic; see Figures 2 and 3, and (19).] Figure 6 illustrates the probability plot for $z(n,i) = u(n,i)^2 + v(n,i)^2$ being chi square in distribution over n (frequency) with i (position) constant when the $u(n,i)$ and $v(n,i)$ matrix ensembles are created with bidirectional autocorrelation using (17)-(21). On this probability plot, we overlay the result before and after rescaling. It is apparent that the $z(n,i)$ matrix ensemble based on rescaled $u(n,i)$ and $v(n,i)$ is nearly chi square over n, but the $z(n,i)$ matrix ensemble based on $u(n,i)$ and $v(n,i)$ before rescaling is much more deviant. Figure 7 illustrates how far outside the Kolmogorov-Smirnov (K-S) 90% confidence limits for being chi square over n with $\sigma_g = .01$ ($\mu = .0002$) the $z(n,i)$ matrix ensemble is before rescaling, and how close it is after rescaling. (The rescaled array very nearly passes the K-S 90% test, especially in comparison to the unscaled array.) All plots discussed in this paragraph and in the rest of this article are based in i (position) unchanging, with statistical manipulations and conclusions referring to n (frequency) dependence, although the same approach would pertain were the roles of the two variables reversed.

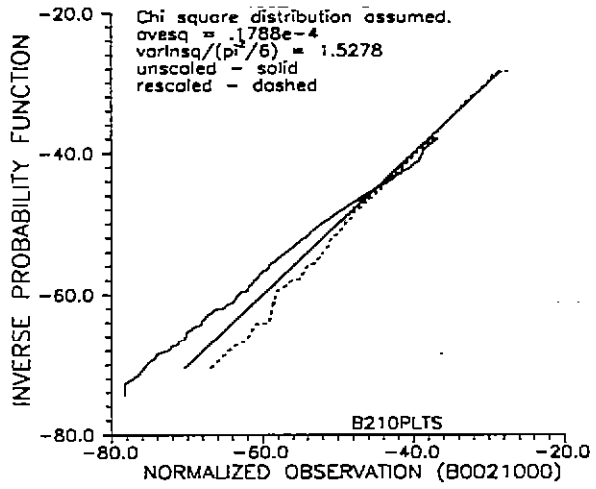

Figure 6. The $z(n,i)$ ensemble has a distribution much closer to chi square after rescaling (dashed) than before (solid).

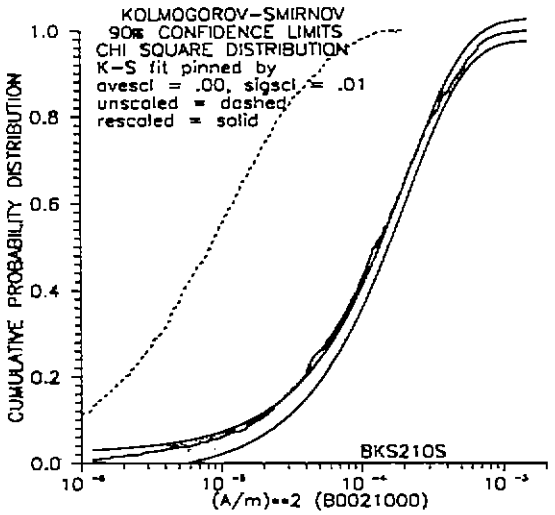

Figure 7. The $z(n,i)$ ensemble is almost brought entirely inside the K-S 90% confidence limits by rescaling.

Summary of Algorithm to Generate the Cable-Drive Field Matrix

Let us now summarize now algorithm for generating the cable-drive fields in an overmoded enclosure. First of all, we need two field-drive matrix ensembles $A(n,i)$ or $B(n,i)$ to represent the two phase-quadrature components of the field at each frequency n and at each cable segment i. These two ensembles are to be completely uncorrelated with each other. The generation procedures for the two ensembles are identical, so we shall only discuss $A(n,i)$. The initial step is to generate a random number matrix having elements $R(n,i)$ uniformly distributed between 0 and 1. The matrix $R(n,i)$ still is to be N x I, so all frequencies and cable segments are represented.

One next maps $R(n,i)$ onto $A(n,i)$ in the manner described by (16) and (17). These particular equations result in an $A(n,i)$ ensemble with a normal distribution having zero mean and σ_g variance. If some other distribution is desired, that distribution should be substituted for the normal in (16) and (17).

The next step is to force local coherence on $A(n,i)$ as functions of n (frequency) and i (position). This coherence should approximately replicate (18) and (19) (see Figures 3 and 4), although we have found the results with respect to simulated cable current response to be quite forgiving if these two correlation formulas are not precisely matched. It is only important that the central lobe of the autocorrelation function be approximately the same width as that experimentally observed or suggested by (18) and (19). Equations (20) and (21) describe one transformation which can be used on $A(n,i)$ to enforce this autocorrelation. Values around 10 usually work for f_{space} and f_{freq}.

This enforced transformation will distort the original distribution placed on the original $A(n,i)$ matrix. It is thus necessary to restore this distribution. Use of (23) and (24) will accomplish this. If one decides that a distribution other than normal is desired, at this point, one needs only substitute the alternative inverse cumulative distribution for $\Phi_g^{-1}(f_m)$ in (24).

Especially if f_{space} and f_{freq} are chosen smaller than 10, application of (24) may destroy some of the autocorrelation. In this case, one iterates the generation of $A(n,i)$ by reapplying (20) and (21), and then (23 and (24). This iteration process may be cycled until further iteration no longer alters the $A(n,i)$ matrix ensemble. Up to 50 iterations are required for very small f_{space} and f_{freq}.

It may occur that, even after all this work, a small growth trend as a function of n (frequency) will remain on the matrix. If this occurs, the technique for eliminating this trend is subsequently described in (26)-(30).

The major source of difficulty stems from the requirement of producing a given distribution and correlation in both the frequency and spatial dimensions. A simpler approach recommended by Ted Lehman is the use of the Karhunen-Loeve expansion [18] over the spatial dimension for each frequency of interest. While this process achieves the proper distribution and correlation for the drivers in space, their relationship from one frequency to the next is random. This results in predictions that can be compared with measurements from one point to the next at a given frequency, but it doesn't allow comparisons to be made at a point over several frequencies; thus half the predictive power of the approach is ignored. It was felt that as much comparison with experiment should be achieveable with the approach and the two-dimensional distribution/correlation procedure described above was retained.

Resulting Cable Current Responses

The above results give the impression that rescaling fixes the $u(n,i)$ and $v(n,i)$ cable-driver matrix ensembles. Consequently, we next examined the real and imaginary distributions of the phase quadrature components of the simulated EMPTAC cable currents. Figure 8 shows that the cable current quadrature components do not fit a normal probability plot. Figure 9 is a Kolmogorov-Smirnov 90% confidence test of the cable power distribution (after filtering to remove the trend). As anticipated from Figure 8, the cable power distribution does not pass the Kolmogorov-Smirnov test for being chi square, even after being run through a trend-removing filter. Figure 10 shows, however, that the unfiltered cable power distribution is excellently matched by a log normal probability plot. At this point, we considered the fact that we had not introduced any mechanism to put the cable current into thermodynamic equilibrium with the electromagnetic environment. To accomplish this, we computed the radiation resistance per unit length of a cable with centerline h (of 5 cm) over a ground plane and diameter small compared to a wavelength:

$$R = \mu_o \omega \frac{\left[1 - J_o(2kh)\right]}{2} \approx \frac{\mu_o \omega}{2}(kh)^2 = \mu_o \omega \pi^2 \left(\frac{h}{\lambda}\right)^2 \qquad \textbf{(25)}$$

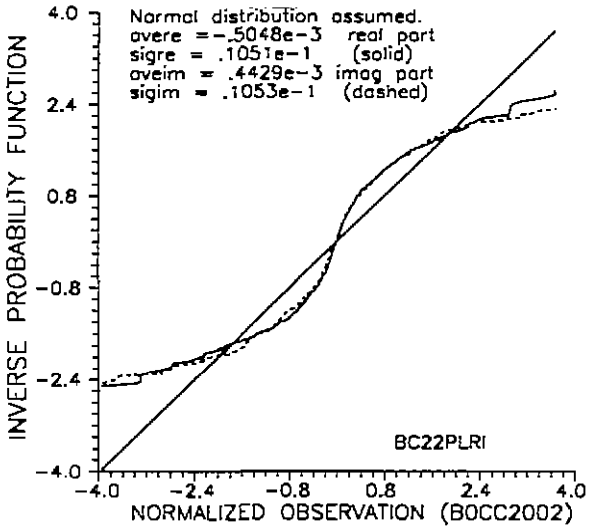

Figure 8. The phase quadrature cable currents resulting from rescaled drive do not fit a normal probability plot.

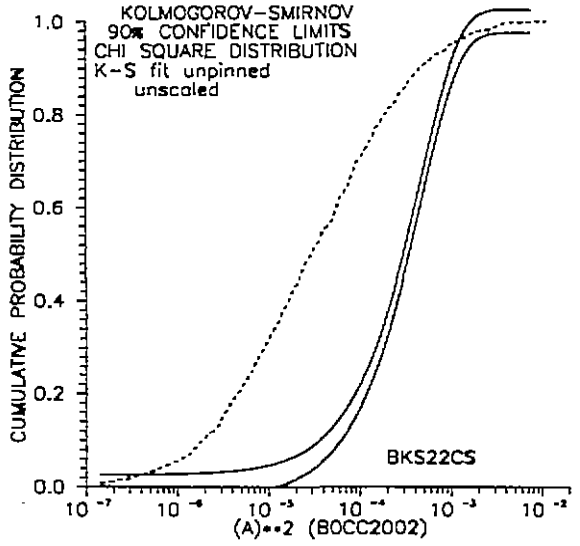

Figure 9. The cable power distribution does not fit a K-S test for being chi square, even after filtering.

The EMPTAC tests we are trying to match were performed with frequency swept from 100 MHz to 1 GHz. At 317 MHz, the above formula leads to a radiation resistance of 120 Ω/m. Consequently, this resistance was next inserted in our cable model. (Part of the justification for doing this was the knowledge that an actual cable at some fixed observation point only responds [correlates] to the driving field over a range of a wavelength or two. Another method to this madness invokes reciprocity: if the cables cannot radiate fields, fields cannot couple to and drive the cables.) Figure 11 shows a considerable improvement for the resulting cable current quadrature components matching a normal distribution (compare with Figure 8). Also, the cable power distribution with trend removed is now closer to being chi square (compare Figure 12 with Figure 9), although it still leaves much to be desired. The unfiltered cable power distribution does still look much more log normal than chi square, however (see Figure 13).

After all the above procedures had been carried out, a tendency (trend) for the cable drive amplitude, and resulting cable current amplitude to grow with frequency was still present. This trend was eventually traced back to the cable drive-field generating equations (17)-(21). We observed that if the drive-field advance equations were made over constant frequency increments (Δf, $\lambda^2/(L\Delta\lambda)$ constant), this equation could not contribute to this drive amplitude shifting: Previously, we had always used an exponentially expanding Δf. Making Δf constant implies that the relative proportions of old and new values, i.e., the effective f_{freq}, cannot change during the generation of the drive-field ensembles.

A similar procedure cannot reasonably be applied to the equation which advances the drive-field along the position axis, as keeping $(\lambda/\Delta l)$ constant requires using a different cable segmenting scheme (different Δl) at every frequency.

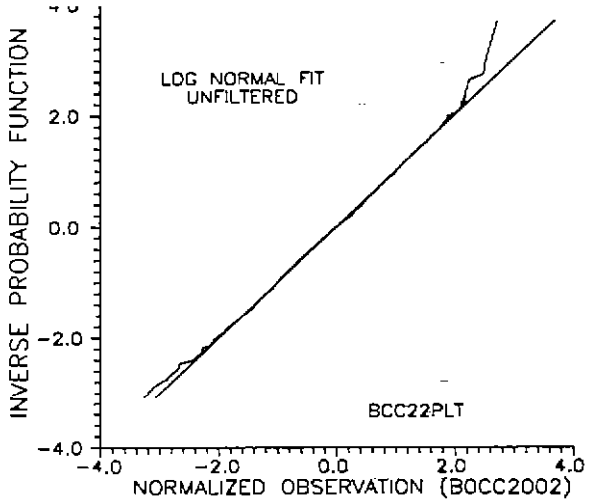

Figure 10. The unfiltered cable power distribution has an excellent match to a log normal probability plot.

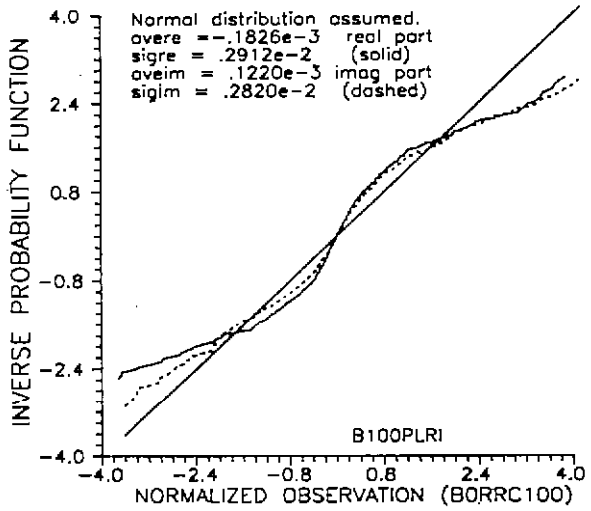

Figure 11. Addition of radiation resistance makes the phase quadrature cable current components more normal.

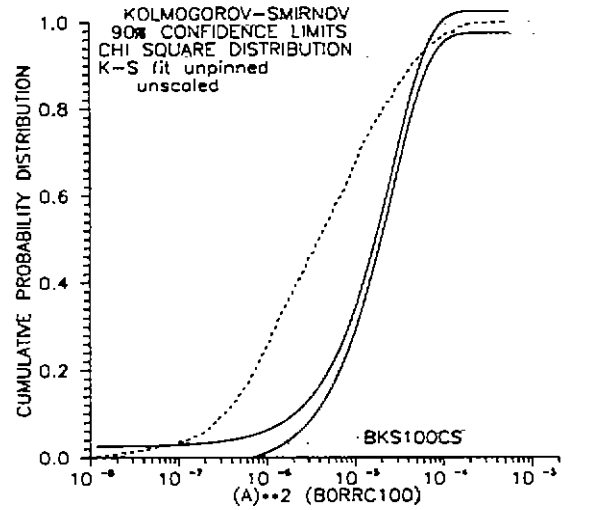

Figure 12. Introduction of radiation resistance brings the filtered cable power distribution closer to being chi square.

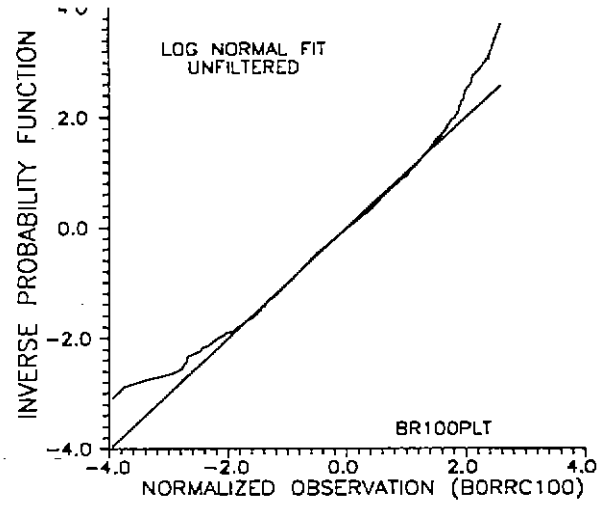

Figure 13. Introduction of radiation resistance leaves the cable power distribution very nearly log normal.

This additional precaution leads to an even more improved (but still not perfect) approach of the *u* and *v* ensembles to a normal distribution (compare the probability plots of Figure 14 with those of Figures 8 and 11). Also, the filtered cable power distribution now approaches chi square much more closely (compare Figure 15 with Figures 9 and 12). Moreover, the unfiltered cable power distribution finally begins to pull away from the ubiquitous log normal form (compare Figure 16 with Figures 10 and 13).

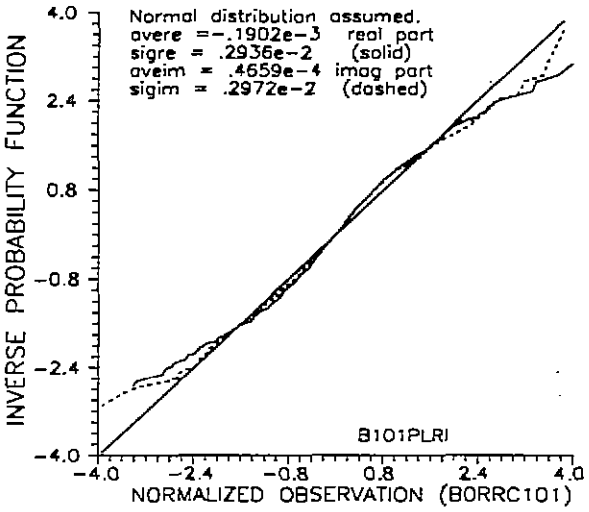

Figure 14. Constant Δf drive-field generation brings the cable quadrature currents still more into normal agreement.

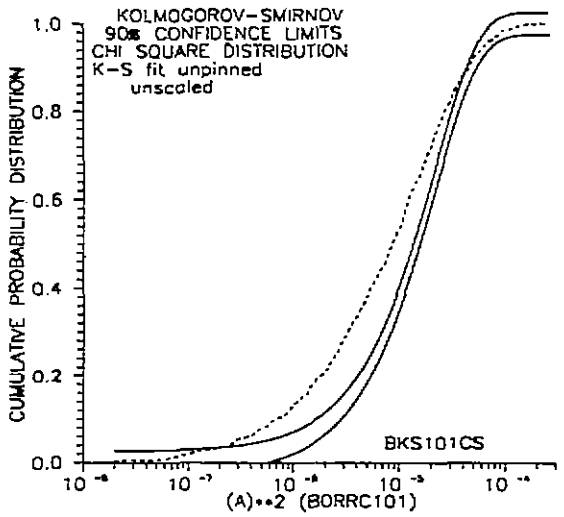

Figure 15. Constant Δf drive-field generation brings cable power distribution still more into a chi square fit.

There is still some growth trend remaining on the $u(n,i)$ and $v(n,i)$ magnetic field matrices as a function of frequency, however (see Figure 17). The last of this growth trend is removed by fitting the absolute magnitudes of the all the local extrema (all points with magnitudes of $u(n,i)$, $U_{ext}(n,i)$, which are both preceded and followed along n by points of lesser magnitude) to a least-squares linear fit: if $U_{ext}(n,i)$ is made to match

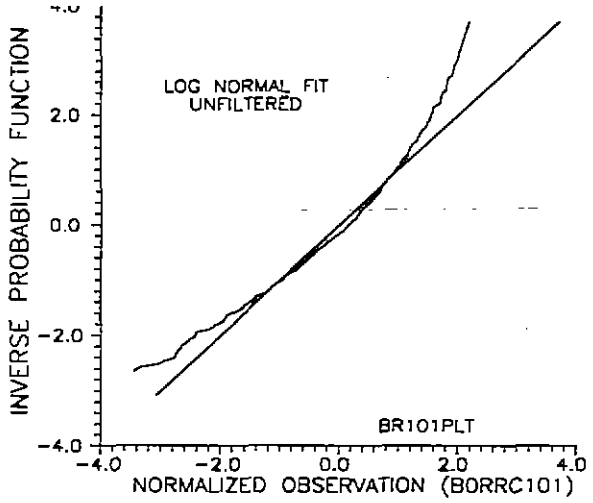

Figure 16. Constant Δf drive-field generation finally causes the cable power distribution to deviate from log normal.

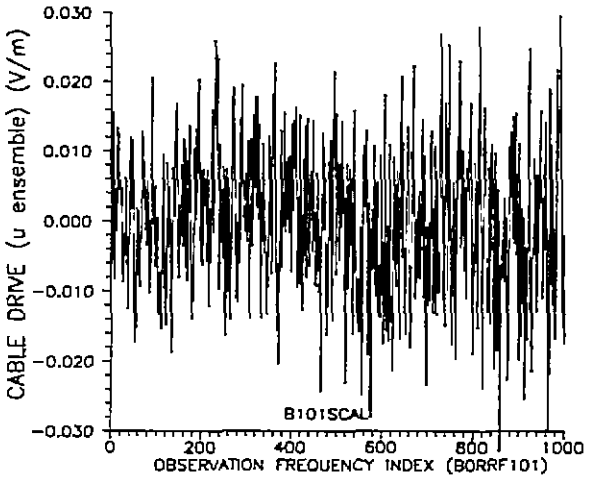

Figure 17. The amplitudes of the $u(n,i)$ ensemble members still have a growing trend as frequency increases, even with constant Δf.

$$U_{ext}(n,i) = \alpha_i f_n + \beta_i \tag{26}$$

in a least-squares sense, one minimizes

$$S_i = \sum_{n \text{ at ext}} (U_{ext}(n,i) - \alpha_i f_m - \beta_i)^2 \tag{27}$$

and finds

$$\alpha_i = \frac{\sum_{n \text{ at ext}} (U_{ext}(n,i) - \overline{U}_{ext}(i))(f_n - \bar{f})]}{\sum (f_n - \bar{f})^2}$$

$$\beta_i = \overline{U}_{ext}(n,i) - \alpha_i \bar{f} \tag{28}$$

In (26)-(28), note is made that $U_{ext}(n,i)$ does not exist at all n, only at n values of locally maximal $U_{ext}(n,i)$. Also, quantities with an overhead bar represent quantities averaged over n (frequency). One then pivots all the points in the ensemble about the center frequency f_c

$$(u(n,i)' - \overline{u(i)}) = (u(n,i) - \overline{u(i)}) \cdot (u_c(i))/u(n,i)) \tag{29}$$

and obtains a new driver ensemble matrix $u(n,i)'$

$$u(n,i)' = \overline{u(i)} + \frac{(u(n,i) - \overline{u(i)})(\alpha_i f_c + \beta_i)}{\alpha_i f_n + \beta_i} \tag{30}$$

This forces the extremal points envelope to lie in a flat line with other points placed between them in appropriate ratios. In this way, we finally compel $u(n,i)$ and $v(n,i)$ to become trendless (see Figure 18). Upon applying the pivoted cable drivers to the cable model, we obtained cable quadrature currents with even better fits to the normal probability plots (see Figure 19). Also, the cable power distribution induced by the pivoted drivers comes still closer to passing a 90% Kolmogorov-Smirnov confidence test for being chi square (see Figure 20).

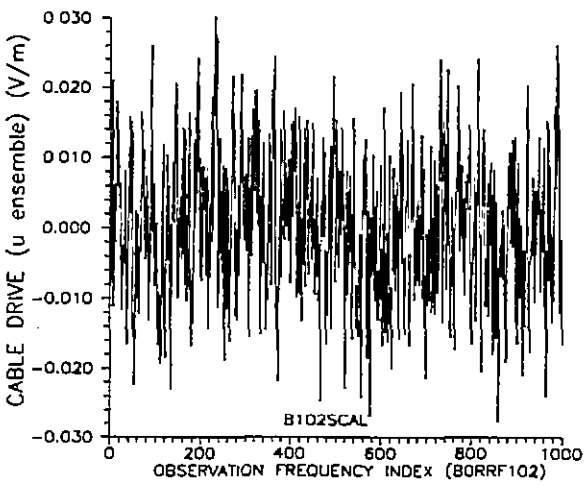

Figure 18. Pivoting ensemble envelopes about average values finally eliminates the cable drivers' growth trend.

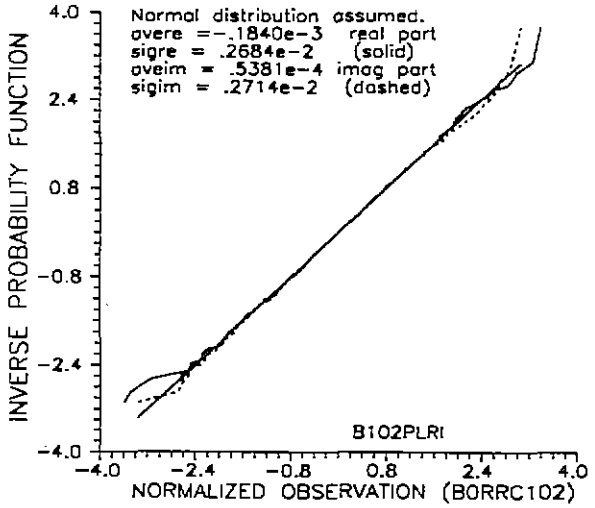

Figure 19. The pivoted cable current drivers actually yield normally distributed phase quadrature cable currents.

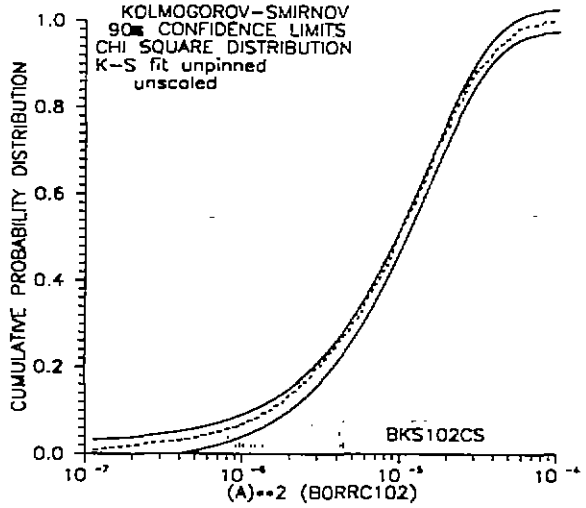

Figure 20. The pivoted cable current drivers actually yield normally distributed phase quadrature cable currents.

Conclusions

An electromagnetic enclosure driven well into the overmoded regime will have a power flux distribution which (as seen by a dipole antenna) is chi square with two degrees of freedom if the observer is fixed and frequency is swept, or if the frequency is fixed and the sensor is translated or rotated. The same power distribution will also be seen incident on cables and conductors within the enclosure. To obtain this distribution, the enclosure must not have a frequency-dependent Q or shielding which varies throughout the enclosure volume. If either of these (or similar) situations occur, the power and power flux distribution densities generally distort towards being log normal.

(There are two mutually exclusive schools of thought as to why the cable powers should have a chi square distribution. Karzas [19] has claimed that the cables effectively sum the incident electric fields all along the cables, and thus the Central Limit Theorem applies to the phase-quadrature cable current components. We think this argument has a flaw: it does not pertain in the presence of radiation resistance that all illumination points on a cable contribute equally to the resulting driven current, irrespective of the separation between the drive point and the current observer. By reciprocity, in the absence of radiation resistance (no feedback from the cable currents to the chamber fields), the chamber fields could not couple to and drive the cables.

(It is our belief, on the other hand, that for a cable in a more-or-less statistically uniform field environment, radiation resistance prevents a cable current from being influenced by fields on the cable at a distance of more than a wavelength or two. If this is the case, the chi square nature of the driving field is immediately and locally transferred to the cable current. Moreover, the Karzas theory leads to cable powers which depend directly on the square root of the cable length [19]. Our theory leads to cable powers which are independent of the cable length past a wavelength or two: this second result is what one normally sees from electromagnetic cable tests.)

This entire set of statistical phenomena may be numerically simulated provided one is very, very careful. For instance, one cannot merely apply normally distributed random electric fields (which correspond to chi square power fluxes) to drive the cables and conductors. The cable-drive fields must be generated so they are additionally endowed with local autocorrelation along spatial and frequency axes as seen in actual experimental data. Also, it is necessary to put a radiation resistance per unit length on the cable to simulate factors which put the cable and the enclosure into electromagnetic thermodynamic equilibrium. Additionally, one must be cautious that the cable-drive fields are free of all trends, including those which may arise from the process of enforcing a local autocorrelation onto the cable-drive field ensemble.

References

[1] R. H. Price, H. T. Davis, and E. P. Wenaas, "Determination of the statistical distribution of electromagnetic-field amplitudes in complex cavities," *Phys. Rev. E*, Vol. 48, December 1993, pp. 4716-4729.

[2] R. H. Price, *et al.*, "Determination of the statistical distribution of electromagnetic field amplitudes in complex cavities," JAYCOR Rep. 88JAL129, June 1, 1988.

[3] B. P. Roe, *Probability and Statistics in Experimental Physics*, New York: Springer-Verlag, 1992 (see, especially, pp. 58-61, pp. 62-63, and pp.189-196).

[4] G. A. Korn and T. M. Korn, *Mathematical Handbook for Scientists and Engineers*, New York: McGraw-Hill, 1968 (see, especially pp. 632-633 and pp. 691-693).

[5] D. A. Hill, "Electronic mode stirring for reverberation chambers," *IEEE Trans. Electromagn. Compat.*, vol. EMC-36, pp. 294-299, November 1994.

[6] R. Holland and R. St. John, "Enforcing correlation on statistically generate EM cable drivers," *Conference Proceedings*, Vol. 1, pp. 308-320, 11th Annual Review of Progress in Applied Computational Electromagnetics, Monterey, CA, 20-25 March 1995.

[7] I. S. Gradshteyn and I. M. Ryzhik, *Tables of Integrals, Series, and Products*, New York: Academic Press, 1965 (see, especially p. 573, Eq. 4.331.1.)

[8] R. Holland and R. St. John, "Statistical responses of enclosed systems to HPM environments," *Conference Proceedings*, Vol. 2, pp. 554-568, 10th Annual Review of Progress in Applied Computational Electromagnetics, Monterey, CA, 21-26 March 1994.

[9] J. G. Kostas and B. Boverie, "Statistical models for a mode-stirred chamber," *IEEE Trans. Electromagn. Compat.*, vol. EMC-33, pp. 366-370, November 1991.

[10] R. R. Lentz and H. C. Anderson, "Reverberation chambers for EMC measurements," presented at the IEEE EMC Symposium, pp. 152-159, 1985.

[11] P. Corona, *et al.*, "Magnification factors for mode stirred chambers," *IEEE Trans. Electromagn. Compat.*, vol. EMC-18, pp. 54-59, May 1976.

[12] R. Lupton, Statistics in Theory and Practice, Princeton: Princeton University Press, 1993 (see, especially, p. 10 and p. 37).

[13] D. A. Hill, *et al.*, "Aperture excitation of electrically large, lossy cavities," *IEEE Trans. Electromagn. Compat.*, vol. EMC-36, pp. 169-178, August 1994.

[14] R. Holland and R. St. John, "Statistical HMP Satellite Survivability Modeling," PL-TR-96-1181, Air Force Phillips Laboratory, Kirtland Air Force Base, NM, November 1996.

[15] D. A. Hill, "Spatial correlation function for fields in a reverberation chamber," *IEEE Trans. Electromagn. Compat.*, vol. EMC-37, p. 138, February 1995.

[16] T. H. Lehman and R. M. Marshall, "Application of statistical physics to derivation of stress and strength distributions," Ball Systems Engineering Division, Albuquerque, NM, September 26, 1991.

[17] T. H. Lehman, "A statistical theory of electromagnetic fields in complex cavities," Air Force Phillips Laboratory, Interaction Note 494, May 1993.

[18] E. J. Johnson, "Constructions of Particular Random Processes," *Proc. IEEE*, pp. 270-285, February, 1994.

[19] W. J. Karzas, "Back door coupling of RF (microwave) energy to space craft interior cabling," Air Force Phillips Laboratory, Interaction Note 513, February 1994.